INSTITUTE OF PHYSICS PUBLISHING JOURNAL OF PHYSICS D: APPLIED PHYSICS

J. Phys. D: Appl. Phys. **39** (2006) 2282–2288 doi:10.1088/0022-3727/39/10/043

Influence of oxygen pressure on the structural and dielectric properties of laser-ablated $Ba_{0.5}Sr_{0.5}TiO_3$ thin films epitaxially grown on (001) MgO for microwave phase shifters

X H Zhu[1], **Q D Meng, L P Yong, Y S He, B L Cheng and D N Zheng**

Beijing National Laboratory for Condensed Matter Physics, Institute of Physics, Chinese Academy of Sciences, Beijing 100080, People's Republic of China

E-mail: xhzhu@ssc.iphy.ac.cn

Received 1 February 2006
Published 5 May 2006
Online at stacks.iop.org/JPhysD/39/2282

Abstract

Highly oriented $Ba_{0.5}Sr_{0.5}TiO_3$ (BST) thin films were grown on MgO (001) single-crystal substrates by pulsed-laser deposition at 800 °C in oxygen pressure ranging from 1.2×10^{-3} to 40 Pa. A strong correlation was observed between the growth process, structure and dielectric properties for the BST films. The dielectric properties in the low frequency range 10 k–1 MHz were measured in the interdigital capacitor configuration. The tetragonal distortion (ratio of in-plane and surface normal lattice parameters, $D = a/c$), surface morphology and dielectric response of the films are strongly dependent on the oxygen deposition pressure. With increase in oxygen pressure, the in-plane strain for the BST films changes from compressive to tensile. The BST film grown at 25 Pa exhibits the best overall dielectric properties. This corresponds to the film with a slight in-plane tensile strain ($D = 1.0012$). It is believed that a reasonable tensile strain, which increases the ionic displacement and thus promotes the in-plane polarization in the field direction, could enhance the tunability and dielectric constant. Based on the BST film grown at 25 Pa, distributed phase shifters were successfully fabricated with promising performance. The phase shifter shows a relatively low insertion loss of about 3.5 dB at zero bias and 10 GHz, a good return loss better than −15 dB for all phase states from dc to 16 GHz and a differential phase shift of about 43° with 120 V dc bias at 10 GHz.

(Some figures in this article are in colour only in the electronic version)

1. Introduction

Barium strontium titanate ($Ba_xSr_{1-x}TiO_3$, hereafter designated as BST) thin films have attracted a great deal of attention because of their potential applications in electrically tunable microwave devices, such as frequency-agile filters, voltage-controlled oscillators, phase shifters and antennae [1–4]. The tunable microwave devices based on ferroelectric films are fast, small and lightweight and, because they work using an electric field, have low power consumption. Their working principle is directly associated with the large variation of dielectric constant in ferroelectric thin films by applying a dc electric field, and this dielectric nonlinearity is the nature of a ferroelectric material. For example, in a phase shifter with a simple coplanar

[1] Author to whom any correspondence should be addressed.

line structure patterned on a ferroelectric thin film coated substrate, the phase velocity of the electromagnetic wave that passes through the coplanar line is controlled by the applied electric field. That is the permittivity of the ferroelectric film is greatly changed by the electric field, which in turn controls the wave velocity and thus the phase can be substantially shifted. As far as these applications are concerned, a good dielectric tunability, defined as $[\varepsilon(0) - \varepsilon(E_{max})]/\varepsilon(0)$, and a low dielectric loss are two prerequisites for BST thin films. Here, $\varepsilon(0)$ is the dielectric constant measured with no bias and $\varepsilon(E_{max})$ is the one measured at the maximum applied bias field. As is well known, one remarkable advantage of MgO single crystal is its extremely low dielectric loss and favourable dielectric constant at microwave frequencies. This makes MgO serve as an excellent substrate for the growth of ferroelectric thin films with the aim of use in tunable microwave device applications. It should be pointed out here that some other single crystals, such as sapphire and $LaAlO_3$, are also frequently used as substrates in ferroelectric film-based microwave components, whereas the standard Si wafers do not provide lattice matching to the perovskite ferroelectrics, resulting in inferior properties of the deposited ferroelectric films, which means that a complicated buffer layer is inevitably required; another problem with the use of Si as substrate for tunable devices is the too high conductivity of poly-Si. As for MgO substrates, there is, however, a large lattice misfit between BST and MgO. For instance, the lattice parameter for bulk $Ba_{0.5}Sr_{0.5}TiO_3$ and MgO is 0.3947 [5] and 0.4212 nm [2], respectively, and the lattice mismatch can be calculated as high as 6.3%. Hence, it is challenging work to grow epitaxially high-quality BST thin films on MgO due to the fact that too large a lattice mismatch can drastically influence the epitaxial quality of thin films by introducing a great number of misfit dislocations and/or charged defects to relieve the lattice-mismatch induced strain. Besides, oxygen pressure during the film deposition plays an important role in tailoring structural and electrical properties of oxide thin films [2,6]. Some experimental results concerning the oxygen pressure dependence of BST thin films have been reported in the literature [7–15]. Nonetheless, the range of oxygen pressure modulation still needs to be widened, especially for the cases of low pressure. Then, the strain effect induced by oxygen vacancies could be well clarified. Furthermore, a systematic investigation of the process–structure–property relationships is of great technological significance. Although BST material shows potential applications in tunable microwave devices, few practical devices have been developed so far due to the fact that the dielectric properties of thin films are drastically inferior to those of their bulk counterpart. Therefore, more work should be performed to push BST thin films further for practical applications.

In this article, we report systematic studies on the influence of oxygen pressure on the structural and dielectric properties of $Ba_{0.5}Sr_{0.5}TiO_3$ thin films epitaxially grown on (001) MgO by pulsed-laser deposition (PLD). The results are explained in terms of the film strain, and the strain is controlled by oxygen vacancies that are regulated by changing the oxygen deposition pressure. The best dielectric properties are obtained in the film with a moderate in-plane tensile strain. Based on this film, a distributed phase shifter is successfully developed and the device characterization is presented.

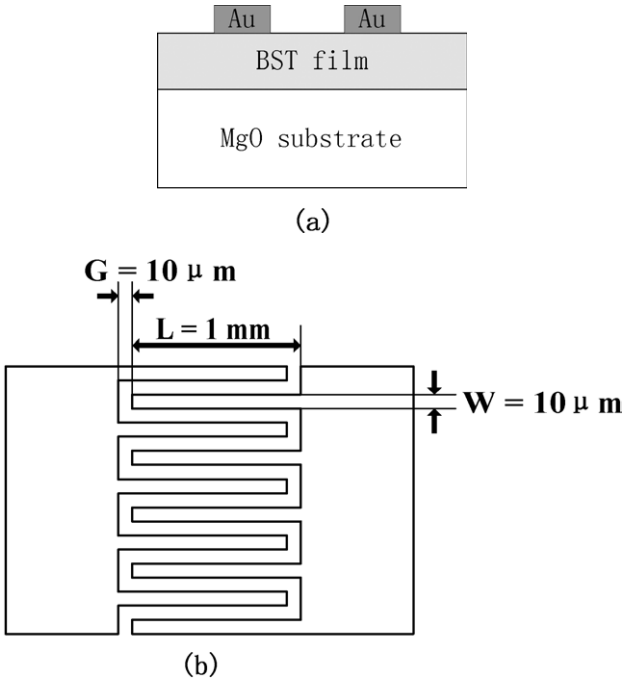

Figure 1. Schematic diagram of the fabricated and investigated devices: (*a*) cross section and (*b*) layout of the interdigital capacitor. Note that the drawing is not to scale.

2. Experimental

Epitaxial $Ba_{0.5}Sr_{0.5}TiO_3$ thin films were grown on (001) MgO single-crystal substrates by PLD using a KrF (248 nm wavelength) excimer laser system (Lambda Physik LPX 300 cc) with a repetition rate of 4 Hz and 25 ns in pulse duration. The pulsed-laser beam was focused by a quartz lens onto a stoichiometric ceramic target with energy density of approximately 1.5 J cm^{-2}. The oxygen pressure in the deposition chamber was maintained at a fixed value in the range 1.2×10^{-3}–40 Pa for each deposition, while the substrate temperature was maintained at 800 °C. The thickness of the BST films was about 350 nm. After each deposition, 1 atm high-purity oxygen was introduced into the growth chamber, the as-deposited film was annealed at 550 °C for 30 min and then slowly cooled to room temperature.

The crystallographic structures of the films were analysed by x-ray diffraction (XRD) using a characteristic x-ray of Cu Kα. The lattice parameters of the BST films were calculated from the symmetric (002) and asymmetric (024) diffraction peaks. Diffraction from the MgO substrate was used as an internal standard to reduce errors associated with measurement. In addition, each BST diffraction peak was fitted with Gaussian functions after removing the background in order to lower the uncertainty as far as possible [9]. The surface morphology of the BST films was characterized by atomic force microscopy using a contact mode (Nanoscope IIIa, DI Multimode SPM).

For dielectric property measurements, the interdigital capacitor technique was used. Figure 1 shows the schematic diagram of the fabricated and investigated devices. Note that the drawing is not to scale for convenience of the eye. Firstly, about 100 nm-thick Au thin film was deposited by dc

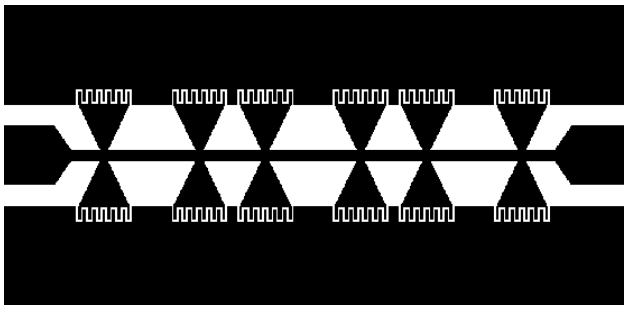

Figure 2. Sketch of the key part for our distributed microwave phase shifter. The finger length is 85 μm, width 17 μm and spacing gap 17 μm for each interdigital capacitor included in the device.

magnetron sputtering. Secondly, the as-grown Au film was annealed in air at 300 °C for 3 h. Lastly, the Au film was etched into the required interdigital electrodes by photolithography. The interdigital capacitor reported here consists of 50 fingers that are 1 mm long, 10 μm wide and spaced 10 μm apart. The measurements were carried out on this pair of coplanar Au interdigital electrodes with an Agilent 4294A Precision Impedance Analyzer. The dielectric constant was extracted from the capacitance by using the conformal mapping results of Gevorgian *et al* [16, 17]. Distributed microwave phase shifters were fabricated using BST interdigital capacitors with 2 μm thick Au film as the top electrode for room temperature operation [18]. A sketch of the key part for our distributed microwave phase shifter is depicted in figure 2. The finger length is 85 μm, width 17 μm and spacing gap 17 μm for each interdigital capacitor included in the device. The device characterization was conducted using an HP 8510C network analyzer at frequencies from dc up to 20 GHz.

3. Results and discussion

Figure 3 shows symmetric (002) and asymmetric (024) XRD θ–2θ scans for the BST films grown on MgO with different oxygen pressures. Pure single-oriented perovskite phase was successfully obtained in all the thin films. As the oxygen deposition pressure increases from 1.2×10^{-3} to 40 Pa, the peak positions of the BST films are shifted to a higher angle, indicating that the lattice parameter of the thin films decreases gradually with the increase in oxygen pressure. Accordingly, the calculated lattice parameters a (along in-plane) and c (along surface normal direction) for the BST films are shown in figure 4(a) together with the calculated tetragonal distortion of thin films ($D = a/c$). Generally, films deposited at higher oxygen pressures show $a > c$ ($D > 1$), while films deposited at lower oxygen pressures show $a < c$ ($D < 1$) [9]. It is proposed that the oxygen vacancies regulated by changing the oxygen deposition pressures are used to control BST film strain [9]. Similarly, we calculated the strain along in-plane of the BST thin films from measured a and c by following $S = (a - a_0)/a_0$, where $a_0 = (a \times a \times c)^{1/3}$. The calculated results of the strain along in-plane and unit cell volume for the BST thin films grown at different oxygen pressures are depicted in figure 4(b). As can be seen clearly from the figure, the film structure is strongly influenced by the oxygen pressure. The unit cell volume of the films increases monotonically with

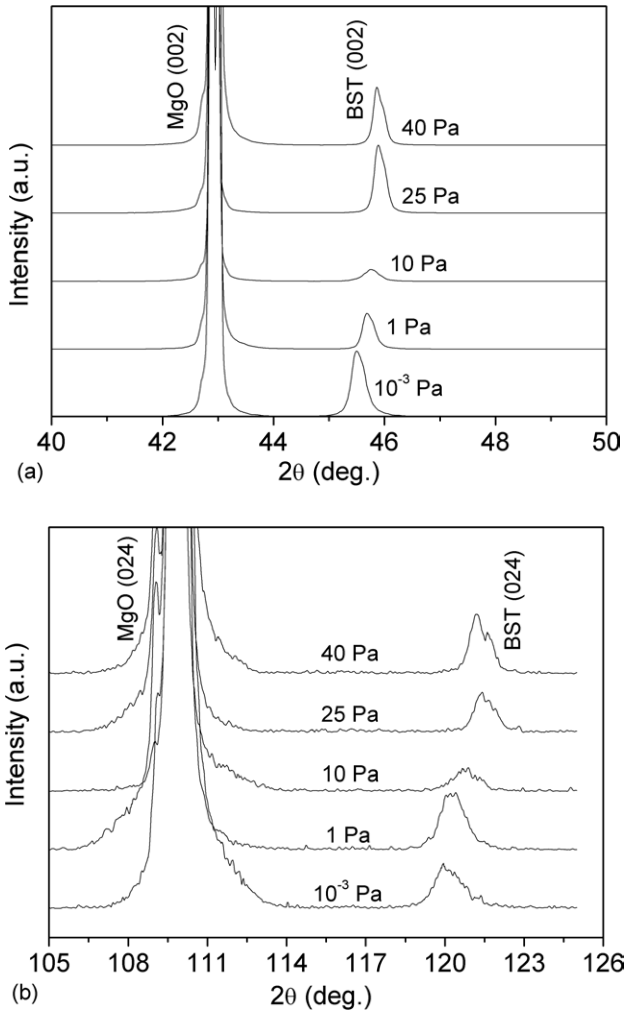

Figure 3. XRD patterns of (a) symmetric (002) and (b) asymmetric (024) peaks of the BST thin films grown on MgO with different oxygen deposition pressures (10^{-3}, 1, 10, 25 and 40 Pa from bottom to top).

decreasing oxygen pressure, revealing higher concentration of oxygen vacancies for the lower oxygen pressure deposited BST films. Oxygen vacancies are considered to affect the nearest neighbour distance by reducing the Coulomb attractive force between cation and anion atoms, resulting in an increased lattice parameter and unit cell volume [8]. Moreover, the in-plane strain changes from compressive to tensile with increasing oxygen pressure. One possible explanation is that the non-isotropic stresses caused by lattice mismatch lead to the change of preferential oxygen vacancy sites between $(0, \frac{1}{2}, \frac{1}{2})$ and $(\frac{1}{2}, \frac{1}{2}, 0)$ due to different activation energies [8, 9]. It is noted that the strain is very large for the two cases of 10 (tensile) and 10^{-3} Pa (compressive) and there is a turnover in 10 Pa.

The microscopic surface morphology of the BST films was investigated by using a contact-mode AFM. Figure 5 shows two-dimensional AFM images of the BST thin films deposited at different oxygen pressures. All the images are measured within a random sample region and the scan area is 2 μm $\times$ 2μm for all. The AFM micrographs indicate that the BST thin films presented in this work are well crystallized, quite smooth and crack free. The root-mean-square (RMS)

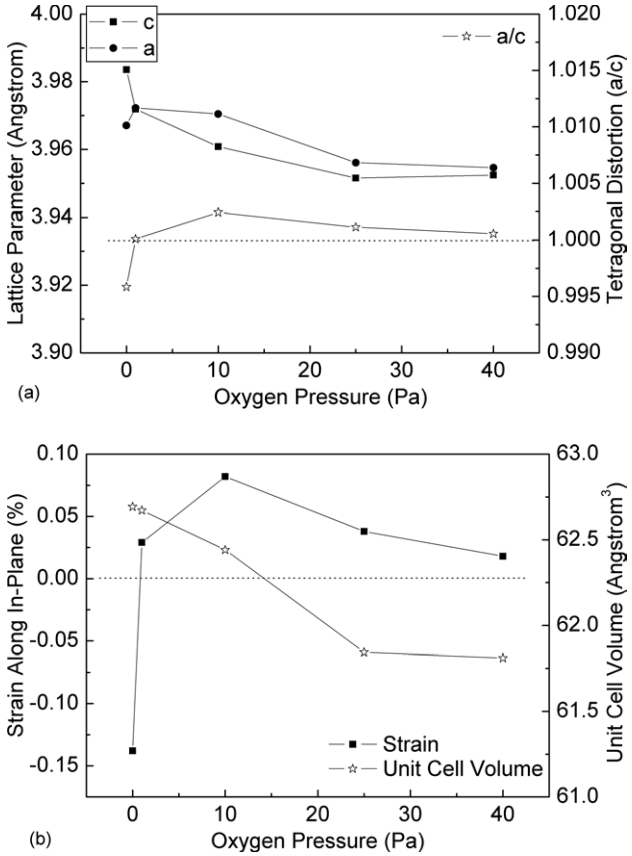

Figure 4. (*a*) In-plane a and surface normal c lattice parameters and tetragonal distortion a/c of the BST films grown on (001) MgO. (*b*) Measured volume of the unit cell and calculated in-plane strain for the BST films grown at different oxygen pressures.

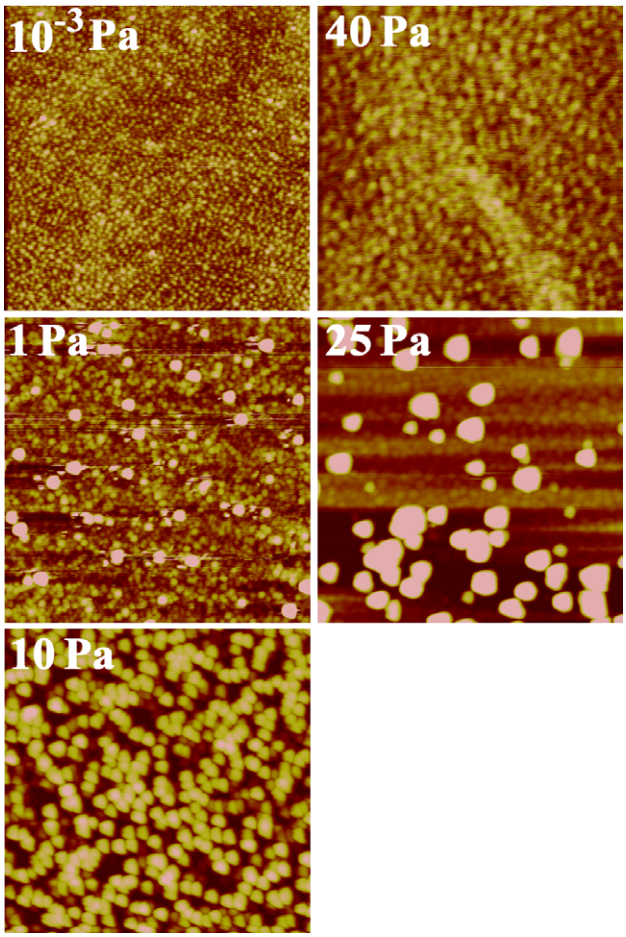

Figure 5. Two-dimensional AFM images of the surface morphology for the BST thin films grown at different oxygen pressures. The scan region is randomly selected and the scan area is 2μm $\times$ 2μm for all.

roughness for the films grown at 10^{-3} and 40 Pa even reaches 0.4 nm, approaching atomic smoothness level. It is very interesting that the grain size of the films gradually increases and the film surface becomes rougher with increase in the in-plane tensile strain (in the order of 10^{-3}–40–1–25–10 Pa). As shown in the figure, furthermore, the densification for the film grown at 10 Pa is relatively worse, probably because an extremely large tensile strain is detrimental to the film growth.

Figures 6(*a*) and (*b*) show the applied electric field dependence of dielectric constant (ε_r) and loss tangent ($\tan\delta$), respectively, for the BST thin films grown at different oxygen pressures, measured at 300 K and 1 MHz. The largest dielectric constant and dielectric tunability is obtained in the film grown at 25 Pa which corresponds to a slight in-plane tensile strain with $D = 1.0012$. Although the dielectric constant is not small for the film grown at 10^{-3} Pa, as the increased unit cell volume and an increased number of oxygen vacancies improve the total polarizability by increasing the number of defect dipoles and the ionic polarizability [8], the dielectric loss in the film is much higher than that in the other films. Furthermore, it suggests a distinct loss mechanism. The dielectric loss problem in the film grown at 10^{-3} Pa is considered to arise from the effect of oxygen vacancies due to the fact that the film deposited in vacuum ambient is extremely oxygen deficient. It should be pointed out that the butterfly-shaped curves indicate a ferroelectric-like hysteresis behaviour in all the films, probably owing both to the oxygen vacancies and to the presence of other space charges, trapped at grain boundaries and/or at the interface [19–21]. For convenience of comparison, the measured dielectric properties at 300 K and 1 MHz for the BST films grown on MgO at different oxygen pressures are summarized. Figures 7(*a*)–(*d*) show the oxygen pressure dependence of dielectric constant, % tunability with applied dc field of 40 kV cm^{-1}, loss tangent and figure of merit (FOM) (FOM = tunability/$\tan\delta_{0\,\mathrm{kV\,cm^{-1}}}$). The best dielectric properties are obtained in the film grown at 25 Pa. It is suggested that a reasonable in-plane tensile strain could enhance remarkably the electrical properties of ferroelectric thin films. However, too large strain could lower the epitaxial quality of thin films and thus debase their properties, such as the two grown at 10 and 10^{-3} Pa. Similar results are reported by others in both planar and parallel-plate capacitor configurations [1, 22–26]. It has been proposed that an appropriate tensile strain along probing electric field could increase the ionic displacement and thereby promote the strain-induced polarization in the field direction, thus enhancing the tunability and the dielectric constant. The high-quality BST film grown at 25 Pa offers us a good material base for tunable microwave device applications.

Figures 8(*a*) and (*b*) show the frequency dispersion curves of dielectric constant and loss tangent with no bias, respectively, measured at 300 K and in the frequency range

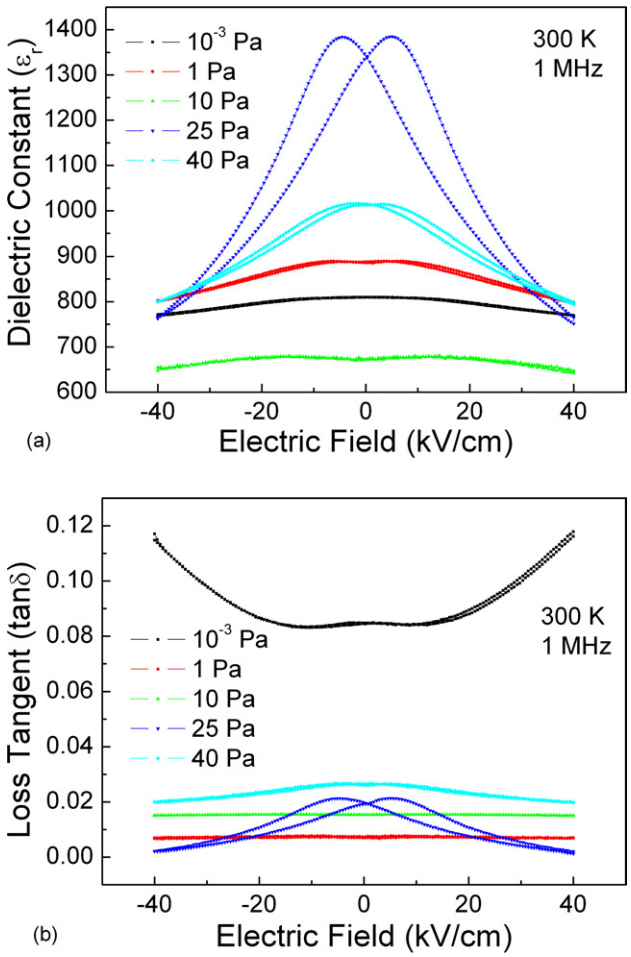

Figure 6. dc electric field dependence of (*a*) dielectric constant and (*b*) loss tangent, respectively, for the BST thin films grown at different oxygen pressures, measured at 300 K and 1 MHz.

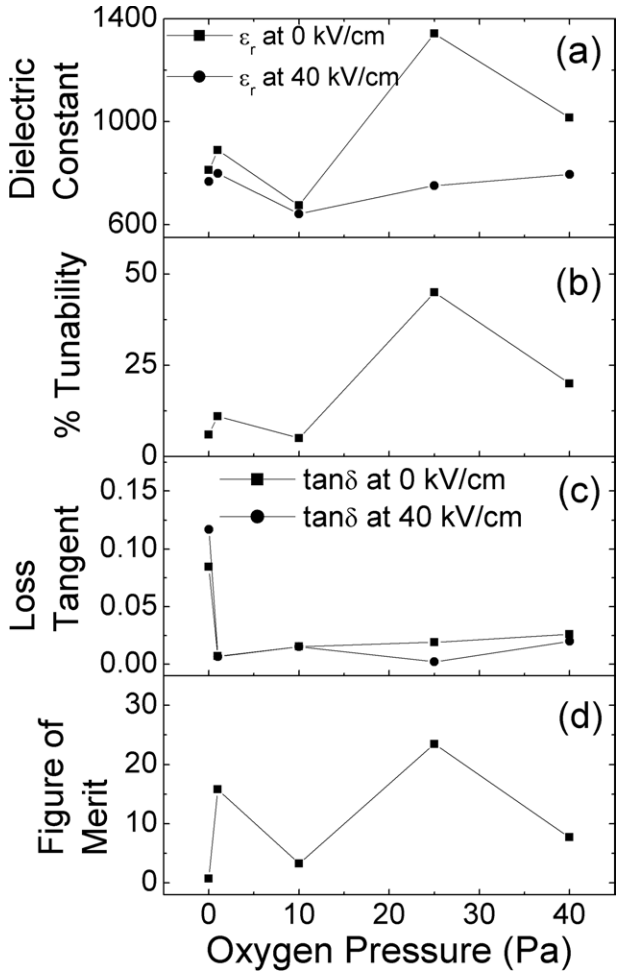

Figure 7. Dielectric properties at 300 K and 1 MHz for the BST films grown on MgO at different oxygen pressures: (*a*) dielectric constant, (*b*) % tunability, (*c*) loss tangent and (*d*) FOM (= tunability/$\tan\delta_{0\,\mathrm{kV\,cm^{-1}}}$).

10 k–1 MHz. The frequency dependence of loss tangent for the four films grown at 1–40 Pa is shown with an inset of figure 8(*b*) for convenience of the eye. As shown in the figures, there is almost no noticeable frequency dispersion for the films grown at normal oxygen pressures ranging from 1 to 40 Pa, indicating the good quality of the films and the absence of internal interfacial barriers [14]. However, the extraordinarily severe dielectric dispersion in the film grown at 10^{-3} Pa is probably attributed to a great number of oxygen vacancies, confirming that an appropriate oxygen deposition pressure is very important for the growth of high-quality BST thin films.

Figure 9 shows the dielectric constant as a function of measurement temperature for the BST thin films grown at different oxygen pressures, measured at 1 MHz. As can be seen from the figure, the temperature of the dielectric constant maximum (T_m) shifts in a wide range for the thin films grown under different conditions. Especially, with respect to the two films grown at 10^{-3} and 10 Pa which are subject to a large strain either compressive or tensile, T_m is over 300 K, much higher than the Curie temperature (T_c) of a perfect $Ba_{0.5}Sr_{0.5}TiO_3$ bulk sample, ∼247 K. According to the results reported in the literature [27, 28], strain in thin films could shift the Curie temperature dramatically. Hence, the shift in T_m is believed to result from the abovementioned strain in our epitaxial BST thin films. Note that the T_m is just below 300 K for the film grown at 25 Pa, ∼291 K. This is a completely favourable characteristic for room-temperature microwave tunable device applications.

The distributed microwave phase shifters are systematically characterized and the measured results are presented in figure 10. As shown in figure 10(*a*), the phase shifter shows very good return loss better than −15 dB for all phase states from dc to 16 GHz, indicating a wide operating frequency range and a good impedance match for circuit designs. The insertion loss is relatively low with a value of about 3.5 dB at zero bias and 10 GHz. It can be decreased significantly by applying a dc bias field. Moreover, the device shows a moderate capability of phase shift with a differential phase shift of about 43° by applying 120 V dc bias at 10 GHz. It should be noted that there is still a large room for improvement in the capability of phase shift by ameliorating the circuit given that the gap size in interdigital capacitors at present is rather large, roughly 17 μm, and can be reduced greatly.

4. Conclusions

Epitaxial $Ba_{0.5}Sr_{0.5}TiO_3$ thin films were grown on MgO (001) single-crystal substrates by PLD at different oxygen pressures

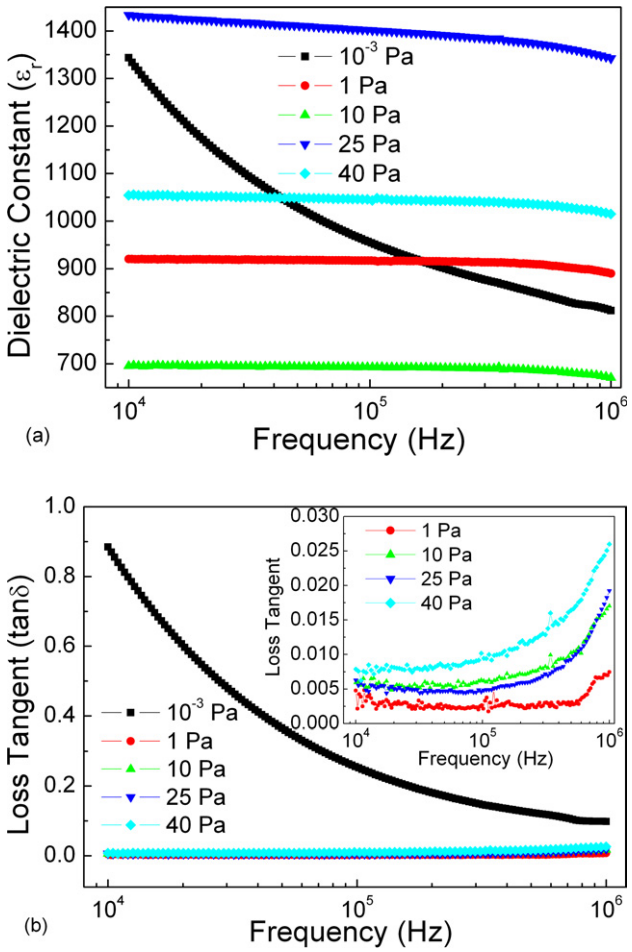

Figure 8. (*a*) Dielectric constant and (*b*) loss tangent as functions of the frequency measured at 300 K. The inset of figure 8(*b*) shows the frequency dependence of loss tangent for the four films grown in oxygen pressure of 1–40 Pa.

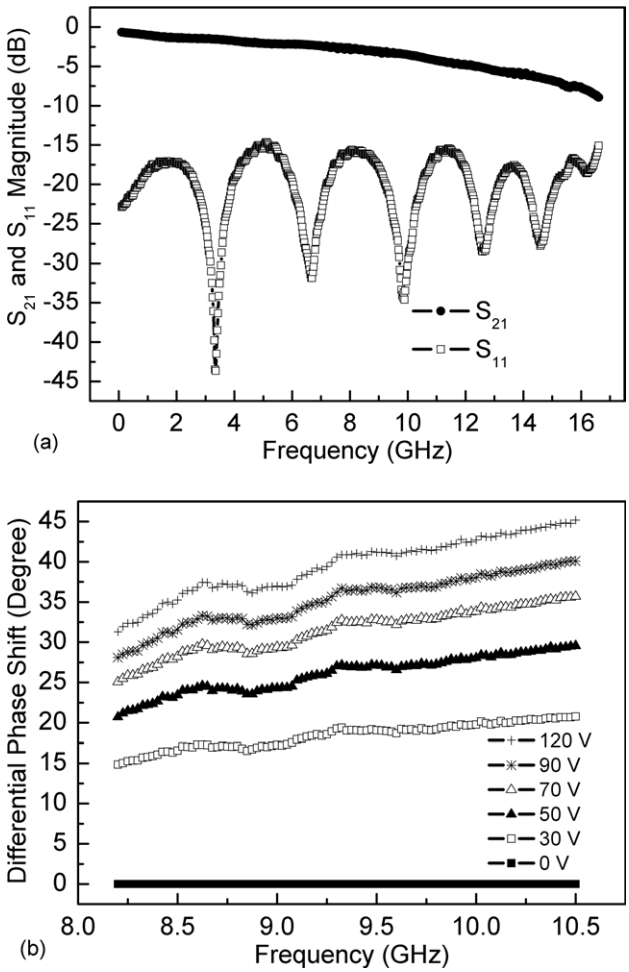

Figure 10. (*a*) Insertion loss and return loss with no dc bias and (*b*) differential phase shift with different dc biases up to 120 V for the distributed phase shifter.

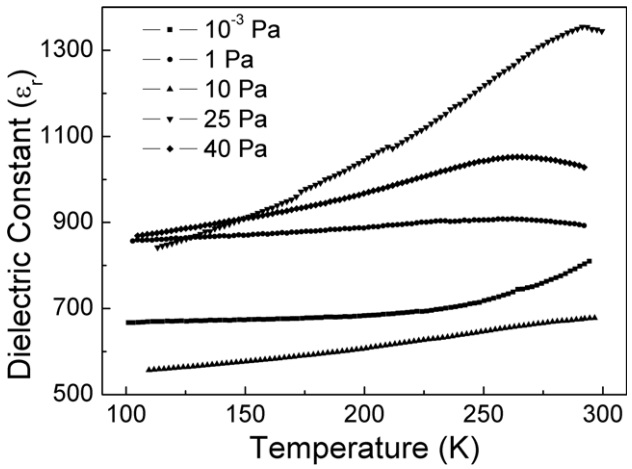

Figure 9. Dielectric constant as a function of the temperature for the BST thin films grown at different oxygen pressures, measured at 1 MHz.

in the range 1.2×10^{-3} Pa–40 Pa. A very strong correlation between the growth process, structure and dielectric properties for the BST films is reported in this work. The film strain can be well controlled by oxygen vacancies that are regulated by changing the oxygen deposition pressure. With increase in the oxygen pressure, the in-plane film strain transforms from compressive to tensile probably due to the change in preferential oxygen vacancy sites between $(0, \frac{1}{2}, \frac{1}{2})$ and $(\frac{1}{2}, \frac{1}{2}, 0)$ caused by the non-isotropic stresses. It is interesting that the film growth and the surface morphology of the BST thin films are adjusted by the film strain. The film grown at 25 Pa, which corresponds to a slight in-plane tensile strain with $D = 1.0012$, shows the largest dielectric constant and dielectric tunability and the best FOM. We believe that a reasonable tensile strain along the probing electric field could increase effectively the ionic displacement and therefore promote the strain-induced polarization in the field direction; however, too large a strain could lower the epitaxial quality of thin films and thus debase their properties. The films grown at normal oxygen pressures for oxide thin film growth exhibit no noticeable frequency dispersion, whereas the film grown in a vacuum of 10^{-3} Pa shows very severe frequency dispersion and a high dielectric loss due to an extremely large number of oxygen vacancies. Furthermore, the temperature of the dielectric constant maximum (T_m) could be remarkably shifted by the film strain. For the film grown at 25 Pa, the T_m is about 291 K, just below 300 K. This is favourable for room-temperature tunable microwave device applications.

Based on the high-quality film grown at 25 Pa, a series of room-temperature distributed microwave phase shifters were successfully fabricated. The device shows a relatively low insertion loss of about 3.5 dB at zero bias and 10 GHz, which can be greatly reduced by applying a dc bias, a good return loss better than −15 dB for all phase states from 0 to 16 GHz and a moderate differential phase shift of about 43° with 120 V dc bias at 10 GHz. There is still a large room for improvement in the device performance by ameliorating the circuit. In summary, the phase shifters exhibit promising prospect for practical applications.

Acknowledgments

This work was financially supported by the National Natural Science Foundation of China (Grant Nos 59832050 and 10174093), the Ministry of Science and Technology of China and the Chinese Academy of Sciences.

References

[1] Carlson C M, Rivkin T V, Parilla P A, Perkins J D, Ginley D S, Kozyrev A B, Oshadchy V N and Pavlov A S 2000 *Appl. Phys. Lett.* **76** 1920
[2] Chen C L, Shen J, Chen S Y, Luo G P, Chu C W, Miranda F A, Van Keuls F W, Jiang J C, Meletis E I and Chang H Y 2001 *Appl. Phys. Lett.* **78** 652
[3] Acikel B, Taylor T R, Hansen P J, Speck J S and York R A 2002 *IEEE Microw. Wireless Compon. Lett.* **12** 237
[4] Cole M W, Nothwang W D, Hubbard C, Ngo E and Ervin M 2003 *J. Appl. Phys.* **93** 9218
[5] Gim Y, Hudson T, Fan Y, Kwon C, Findikoglu A T, Gibbons B J, Park B H and Jia Q X 2000 *Appl. Phys. Lett.* **77** 1200
[6] Zhu X H, Zhu J M, Zhou S H, Liu Z G, Ming N B, Lu S G, Chan H L W and Choy C L 2003 *J. Electron. Mater.* **32** 1125
[7] Nakamura T, Yamanaka Y, Morimoto A and Shimizu T 1995 *Japan. J. Appl. Phys.* **34** 5150
[8] Kim W J, Chang W, Qadri S B, Pond J M, Kirchoefer S W, Chrisey D B and Horwitz J S 2000 *Appl. Phys. Lett.* **76** 1185
[9] Kim W J, Wu H D, Chang W, Qadri S B, Pond J M, Kirchoefer S W, Chrisey D B and Horwitz J S 2000 *J. Appl. Phys.* **88** 5448
[10] Carlson C M, Parilla P A, Rivkin T V, Perkins J D and Ginley D S 2000 *Appl. Phys. Lett.* **77** 3278
[11] Wang Y G, Reeves M E, Kim W J, Horwitz J S and Rachford F J 2001 *Appl. Phys. Lett.* **78** 3872
[12] Navi N, Kim H, Horwitz J S, Wu H D and Qadri S B 2003 *Appl. Phys. A* **76** 841
[13] Ding Y P, Wu J S, Meng Z Y, Chan H L and Choy Z L 2002 *Mater. Chem. Phys.* **75** 220
[14] Goux L, Gervais M, Catherinot A, Champeaux C and Sabary F 2002 *J. Non-Cryst. Solids* **303** 194
[15] Delage T, Champeaux C, Catherinot A, Seaux J F, Madrangeas V and Cros D 2004 *Thin Solid Films* **453–454** 279
[16] Gevorgian S, Carlsson E, Rudner S, Wernlund L D, Wang X and Helmersson U 1996 *IEE Proc. Part H: Microwaves, Antennas Propag.* **143** 397
[17] Gevorgian S S, Martinsson T, Linner P L J and Kollberg E L 1996 *IEEE Trans. Microw. Theory Tech.* **44** 896
[18] Liu Y, Nagra A S, Erker E G, Periaswamy P, Taylor T R, Speck J and York R A 2000 *IEEE Microw. Guided Wave Lett.* **10** 448
[19] Pontes F M, Leite E R, Longo E, Varela J A, Araujo E B and Eiras J A 2000 *Appl. Phys. Lett.* **76** 2433
[20] Hubert C, Levy J, Cukauskas E J and Kirchoefer S W 2000 *Phys. Rev. Lett.* **85** 1998
[21] Xia Y D, Cheng J B, Pan B, Wu D, Meng X K and Liu Z G 2005 *Appl. Phys. Lett.* **87** 052902
[22] Park B H, Peterson E J, Jia Q X, Lee J, Zeng X, Si W and Xi X X 2001 *Appl. Phys. Lett.* **78** 533
[23] Hyun S, Lee J H, Kim S S, Char K, Park S J, Sok J and Lee E H, 2000 *Appl. Phys. Lett.* **77** 3084
[24] Hyun S and Char K 2001 *Appl. Phys. Lett.* **79** 254
[25] Wang D Y, Wang Y, Zhou X Y, Chan H L W and Choy C L 2005 *Appl. Phys. Lett.* **86** 212904
[26] Bellotti J A, Chang W, Qadri S B, Kirchoefer S W and Pond J M 2006 *Appl. Phys. Lett.* **88** 012902
[27] Choi K J *et al* 2004 *Science* **306** 1005
[28] Haeni J H *et al* 2004 *Nature* **430** 758